390

VOLUME 80 SEPARATE No. 390

PROCEEDINGS

AMERICAN SOCIETY OF CIVIL ENGINEERS

JANUARY, 1954

A NEW CONCEPT OF FLOW IN ROUGH CONDUITS

by Henry N. Morris, A.M. ASCE

HYDRAULICS DIVISION

(Discussion open until May 1, 1954)

Headquarters of the Society
33 W. 39th St.
New York 18, N. Y.

PRICE $0.50 PER COPY

THIS PAPER

--represents an effort by the Society to deliver technical data direct from the author to the reader with the greatest possible speed. To this end, it has had none of the usual editing required in more formal publication procedures.

Readers are invited to submit discussion applying to current papers. For this paper the final date on which a discussion should reach the Manager of Technical Publications appears on the front cover.

Those who are planning papers or discussions for "Proceedings" will expedite Division and Committee action measurably by first studying "Publication Procedure for Technical Papers" (Proceedings — Separate No. 290). For free copies of this Separate—describing style, content, and format—address the Manager, Technical Publications, ASCE.

This paper was published at 1745 S. State Street, Ann Arbor, Mich., by the American Society of Civil Engineers. Editorial and General Offices are at 33 West Thirty-ninth Street, New York 18, N. Y.

A NEW CONCEPT OF FLOW IN ROUGH CONDUITS

Henry M. Morris

SYNOPSIS

A new and expanded concept of flow over rough pipe and channel surfaces, based particularly upon the effect of the longitudinal spacing of surface roughness elements and their associated vorticity streams, recognizes three basic types of rough conduit flow. These basic flow types have been denoted as isolated-roughness flow, wake-interference flow, and quasi-smooth or skimming flow.

The friction factor equations derived for these three types of flow appear to be adequately substantiated by data obtained by many different experimenters, on all types of roughnesses, in both pipes and open channels. They can be extended to surfaces of variable roughness, so that reasonably accurate predictions of friction factor can be made for all types of conduit surfaces. The concept is physically reasonable and is relatively simple analytically, so that it appears to bear promise as a more useful and rational method for the hydraulic design of conduits than methods in current use.

Introduction

As a contribution toward the practical solution of the important problem of the hydraulics of flow in rough conduits, a general concept of such flow will here be offered, which is intended to make possible the prediction of friction factors for any type of conduit surface.

The Darcy equation for head loss is as follows:

$$H_f = f \frac{L}{D} \frac{V^2}{2g} \tag{1}$$

where H_f represents the feet of head loss in a length L of the conduit, f is the Darcy friction factor, D is the equivalent diameter of the conduit, and V is the average velocity of flow across any section. The friction factor is a dimensionless coefficient, which can be shown by dimensional analysis to be a function of the Reynolds number of the flow and of several dimensionless geometric ratios. Thus:

$$f = \phi\,(R, h/D, \lambda/D, s/D, - - -) \tag{2}$$

where R is the Reynolds number DV/γ, γ is the kinematic viscosity of the fluid, h is the radial height of the wall roughness projections, λ is the spacing of the wall roughness elements in the direction of flow, and s is the clear peripheral spacing between elements. If other dimensions are necessary to describe the roughness elements, then as many more dimensionless geometric terms should be included in the function ϕ.

The velocity distribution curve in pipes with rough walls has been found experimentally, especially by Nikuradse (11), to fit the following:

$$\frac{v}{v_*} = a + b \log_{10} \frac{y}{r_o} \tag{3}$$

where a is a dimensionless parameter depending on the type of roughness, r_o is the pipe radius, and b is 5.75. The constant 5.75 is actually $\frac{\log_e 10}{k}$, where k is the von Karman universal turbulence constant, which has been shown to be applicable to the interior turbulence of smooth and rough-walled conduits alike, and to have an approximate experimental value of 0.40. The velocity traverses obtained by Nikuradse in his sand-coated pipes are usually described by the following equation:

$$\frac{v}{v^*} = 8.5 + 5.75 \left(\log_{10} \frac{y}{e}\right) \tag{4}$$

where e is the diameter of uniform sand-grains coated on the wall. The corresponding equation for friction factor is:

$$\frac{1}{\sqrt{f}} = 2 \log_{10} \frac{r_o}{e} \quad 1.74 \tag{5}$$

This equation obviously implies f to be independent of R and to be a function solely of the relative roughness $\frac{e}{r_o}$. Thus, this type of flow, commonly known as rough-pipe flow, follows the quadratic resistance law, with the head loss proportional to the square of the velocity.

However, Nikuradse also showed that rough pipes normally will experience a brief regime of smooth-pipe flow at low Reynolds numbers before the roughness projections begin to have a material effect on the turbulence. A transition flow regime is then established between smooth and rough-pipe flow, in which the friction factor first decreases, then increases and finally becomes constant as R increases.

It has often been assumed that all types of conduit surfaces would also give a constant friction factor at sufficiently high values of R. However, most commercial pipe tests have yielded descending f-R curves, with some tests giving horizontal characteristics and very infrequently rising characteristics.

In recent years, the practice of using the Nikuradse equivalent sand-grain diameter, K_s, as a measure of surface roughness, has been increasing among engineers. This term is defined as the sand-grain diameter which would give the same value of friction factor as the actual pipe, obtained by solving eq. (5) for $K_s = e$.

Since, however, most f-R curves for commercial pipes have been found to have descending characteristics throughout the experimental range, the formula of Colebrook and White (2) is often used to determine the value of K_s, or at least to define the transition regime for the surface being tested. This formula is:

$$\frac{1}{\sqrt{f}} = 2 \log_{10} \frac{r_o}{K_s} + 1.74 - 2 \log_{10} \left[1 + \frac{18.7}{\frac{R\sqrt{f}}{r_o/K_s}}\right] \tag{6}$$

This equation gives a curve which is asymptotic to both the Nikuradse smooth and rough-pipe curves. If implies that f decreases as R increases. The parameter $\frac{1}{\sqrt{f}} - 2 \log_{10} \frac{r_o}{K_s}$ has been called by Prandtl the generalized

resistance function and the parameter $\frac{R\sqrt{f}}{r_o/K_s}$ can be shown to be a wall Reynolds number equal to $\frac{v^*K_s}{\gamma} \cdot \sqrt{32}$.

The use of the Nikuradse and Colebrook-White equations, together with the design methods based thereon, undoubtedly represents a substantial improvement in previous design methodology. However, there exist several important deficiencies in this method which it is hoped the concept of the present paper will overcome.

Probably the most important such defect lies in the failure of the Colebrook-White equation to apply to conduit surfaces which produce either horizontal or rising f-R curves. The tests of Harris (5) on surfaces of "random" roughness yielded f-R curves which were essentially horizontal after leaving the smooth-pipe curve. Tests at the St. Anthony Falls Hydraulic Laboratory on commercial corrugated metal culvert pipes (16) revealed a definitely rising characteristic for the f-R relation.

Furthermore, even for pipes which give the usual falling characteristic, experimental values of K_s do not always turn out to be a function of only the type of surface. Tests on concrete pipes at the St. Anthony Falls Hydraulic Laboratory, for example, (14), (15), have implied K_s as computed from the Colebrook-White equation to vary with both R and r_o.

Finally, it is apparent that K_s has no definite physical significance as far as the roughness elements on the surface are concerned, with the exception of uniform sand-coated surfaces. However, its use has often seemed to imply that it is being associated with the height of projection $\underline{h}$ of the elements. There is no reason, of course, why $\underline{h}$ and K_s should be equal or even be correlated with each other, since other roughness dimensions will obviously exert a material effect on the friction factor.

It is thus desirable, if possible, to develop a new concept of rough conduit flow which will utilize a physically realistic measure of surface roughness, and which will be able to explain and predict the different forms of f-R curves, and finally which can predict friction factors for any surface of known roughness dimensions and for any value of Reynolds number.

The Importance of Form Drag and Roughness Spacing

The chief source of friction loss in a fluid flowing over a rough surface is evidently the generation, spreading, and subsequent dissipation of vortices from the wake and separation zone behind each roughness element. Each element is thus a source of vorticity, and the longitudinal frequency with which such sources of vorticity occur is therefore of greatest significance in controlling the turbulence structure and energy dissipation phenomena.

This fact strongly suggests that the longitudinal spacing λ of the roughness elements is the roughness dimension that is of greatest importance in rough conduit flow and would thus offer the most likely basis of correlation of friction loss data in such conduits.

With this in mind, two parameters involving the roughness spacing $\underline{\lambda}$ will be defined for later reference. The <u>roughness index</u> is defined as λ/h, the ratio of the roughness element spacing to the radial height of projection. The <u>relative roughness spacing</u> is defined as r_o/λ, the ratio of radius to roughness element spacing. This term is similar to, but should not be confused

with the ratio usually defined as the relative roughness, r_o/h. The radius r_o, as well as other radial dimensions y, will be measured with reference to a datum through the crests of the roughness elements. This is believed to be the best choice of datum in view of the fact that the wake and vortex-generating zone at each roughness element originates at or near the crest of the element.

Basic Types of Flow in Rough Conduits

Recognizing, then, the fundamental significance of the roughness element spacing in the expenditure of flow energy, it next becomes apparent that three different types of flow phenomena may occur near the wall; the type which occurs in a given situation will depend primarily upon the value of λ for the given roughness.

If the wall roughness elements are far apart, separated by long reaches of relatively smooth wall surface, then the individual elements will act as isolated bodies on which are exerted drag forces by the flowing fluid. The wake and vortex-generating zone at each element is completely developed and dissipated before the next element is reached. The apparent friction factor would therefore result from the form drag on the roughness elements in addition to the friction drag on the wall surface between elements. The form drag on any one element would depend largely on the height of projection h of the element. The total form drag in a given length of a conduit would depend upon λ. Thus, the roughness index λ/h, could be expected to be a significant correlating parameter, for this type of flow, which can be designated as isolated-roughness flow.

The second type of flow results when the roughness elements are placed sufficiently close together so that the zone of separation and vortex generation and dissipation associated with each element is not completely developed before the next element is encountered. This type of flow may be called wake-interference flow, involving as it does the interference by the wake of each element with the vortex spreading and dissipation connected with the preceding element. The friction drag of the wall itself is obliterated, and the entire region near the wall is the scene of intense and complex vorticity and turbulent mixing. The height h of the element is relatively unimportant in this type of flow, but again the spacing λ is obviously of major importance. Also the pipe size will control in part the radial extent of this wall region of abnormal turbulence. For wake-interference flow, therefore, the relative roughness spacing r_o/λ will be an important correlating parameter.

Still another type of flow would result when the roughness elements are so close together that the flow essentially skims the crests of the elements. In the grooves between the elements will be regions of dead water containing stable vortices. The bulk flow will be over a pseudo-wall composed of the roughness crests and the upper limbs of the groove vortices. Large roughness projections will be absent from this pseudo-wall, and the flow will thus be similar to smooth-conduit flow. This type of flow might be called either quasi-smooth flow or skimming flow. Much of the energy loss in such flow can probably be attributed to the maintenance of the groove vortices, the size of which is controlled by the width or the depth of groove, whichever is smaller. The number of such vortices depends on λ. The roughness index, expressed either as λ/h or λ/j, where j is the groove width, can thus be expected to be a significant parameter influencing the apparent friction factor in skimming flow.

Theory of Wake-Interference Flow

The wake-interference flow phenomena will be considered first, primarily because of the fact that the well-known Nikuradse sand-coated pipes seem to have produced this type of flow.

For the purpose of developing general equations descriptive of wake-interference flow, consider a circular pipe section, at a distance sufficiently removed from the entrance or other irregularity to permit full development of the turbulent boundary layer. At each roughness element will be formed a wake, from which vortices will be shed towards the pipe center. The forward velocity of flow will wash the vortices downstream, where they will commingle with the vortices from the next roughness wake. Thus a relatively distinct wall zone of flow will result, in which will prevail a high comparative intensity of turbulent mixing.

In the central region of the pipe, normal turbulence, characterized by the von Karman similarity constant $\underline{k}$, will prevail. The boundary between the central and wall regions will be at a distance from the wall which is probably primarily dependent on the spacing of the elements, since it is this parameter which controls the frequency of vorticity sources and the spread angle of vortices toward the central region. Accordingly, the distance of the boundary between the wall and central zones will be taken as $c\lambda$, where $\underline{c}$ can probably be expected to vary somewhat with the wall Reynolds number and with the relative roughness spacing.

The general dimensionless equation of velocity distribution in the central region is then:

$$\frac{v}{v^*} = a + \frac{1}{k}\left(\log_e \frac{y}{c\lambda}\right) = A + \frac{1}{k}\left(\log_e \frac{y}{\lambda}\right) \tag{7}$$

where v is the velocity at distance y from the roughness crests, and v^* is the friction velocity. The dimensionless number $\underline{a}$ is the value of $\frac{v}{v^*}$ at the boundary between the two regions at $y = c\lambda$, and the number $\underline{A}$ is the value of $\frac{v}{v^*}$ at the distance $y = \lambda$. Note that $\underline{A}$ is also $(a - \frac{1}{k}\log_e c)$.

Because of the higher relative intensity of turbulent mixing in the wall region, the velocity distribution would be expected to be more nearly uniform in this region than would correspond to the von Karman constant $\underline{k}$. The equation of velocity distributions in this wall zone is not known of course, but might reasonably be assumed to be of the same general form as eq. (7) though with a different turbulence parameter replacing $\underline{k}$.

Accordingly, the following velocity distribution equation is postulated for the wall zone:

$$\frac{v}{v^*} = a + \Psi \log_e \frac{y}{c\lambda} = A_w + \Psi \log_e \frac{y}{\lambda} \tag{8}$$

Again, $\underline{a}$ is the value of $\frac{v}{v^*}$ at $y = c\lambda$, the break in the velocity distribution curves, and $\underline{A_w}$ is the value of $\frac{v}{v^*}$ at $y = \lambda$. The parameter Ψ corresponds to $^1/_k$ in the normal velocity distribution equation (7). If $\frac{v}{v^*}$ is plotted against $\log_e \frac{y}{\lambda}$ for a given pipe section, then $^1/_k$ is the slope of the curve for the central region and Ψ is the slope in the wall region. In general the

value of $^1/_k$ must equal or exceed the value of Ψ, because of the abnormal turbulence in the wall zone and therefore the more nearly uniform velocity distribution (when plotted on a semi-logarithmic basis as indicated).

The parameter Ψ is evidently not a constant since it depends upon the wake and vortex-spreading phenomena in the wall region, which depend in turn upon the form and dimensions of the roughness elements (especially their longitudinal spacing) and upon the fluid velocity and viscosity. For a given wall roughness, it is probable that Ψ will prove to be a function of the wall Reynolds number, defined as $\frac{R\sqrt{f}}{r_o/\lambda}$ and of the cross-sectional form of the individual roughness elements, and that, for a given form of element, Ψ will approach $^1/_k$ as the wall Reynolds number, R_w, increases. It is assumed that Ψ does not vary significantly with y. This assumption ignores at least a small transition zone, both near the wall and near the central core zone, but the use of a constant, average, value of Ψ throughout the wall zone will materially simplify the ensuing analysis and will not significantly affect the results.

It is next desirable to obtain an expression for the average velocity of flow through the entire cross-section. This can be done by integrating the elements of discharge across the section, then dividing by the total area. Thus:

$$\frac{V}{v^*} = \frac{\int v dA}{Av^*} = \frac{2\pi \int vrdr}{Av^*}$$

$$= \frac{2}{r_o}\left[\int_0^{c\lambda} (r_o - y)\left(a + \Psi \log_e \frac{y}{c\lambda}\right) dy + \int_{c\lambda}^{r_o} (r_o - y)\left(a + \frac{1}{k}\log_e \frac{y}{c\lambda}\right) dy\right] \tag{9}$$

Omitting the intermediate steps, this expression ultimately reduces to:

$$\frac{V}{v^*} = \left(A - \frac{3}{2k}\right) + \left(\frac{1}{k} - \Psi\right)\left[2\left(\frac{c\lambda}{r_o}\right) - \frac{1}{2}\left(\frac{c\lambda}{r_o}\right)^2\right] + \frac{1}{k}\log_e \frac{r_o}{\lambda} \tag{10}$$

where V is the average velocity of flow over the cross-section. Replacing $\frac{V}{v^*}$ by its equivalent, $\sqrt{\frac{8}{f}}$, the following results:

$$\frac{1}{\sqrt{f}} - \frac{1}{k\sqrt{8}}\log_e \frac{r_o}{\lambda} = \frac{1}{\sqrt{8}}\left(A - \frac{3}{2k}\right) + \frac{1}{\sqrt{8}}\left(\frac{1}{k} - \Psi\right)\left[2\left(\frac{c\lambda}{r_o}\right) - \frac{1}{2}\left(\frac{c\lambda}{r_o}\right)^2\right] \tag{11}$$

This equation may be described as the general resistance equation for axial wake interference flow.

A similar equation may be derived for two-dimensional wake-interference flow in an analagous manner, the final equation being as follows:

$$\frac{1}{\sqrt{f}} - \frac{1}{k\sqrt{8}}\log_e \frac{b}{\lambda} = \frac{1}{\sqrt{8}}\left(A - \frac{1}{k}\right) + \frac{1}{\sqrt{8}}\left(\frac{1}{k} - \Psi\right)\left(\frac{c\lambda}{b}\right) \tag{12}$$

where $\underline{b}$ is the distance from the roughness crests to the channel center.

The left-hand member of equations (11) and (12) will be referred to as the resistance function. The first term in the right-hand member is the lower limiting value of the resistance function. The second term in the right-hand member is the corrective term, which approaches and eventually reaches

zero at high values of the wall Reynolds number, since ψ approaches $^1/_k$ and $\underline{c}$ decreases as R_w increases.

The term k is the universal turbulence constant of von Karman, usually taken to be about 0.40, although there is considerable evidence that a more generally accurate value would be about 0.37 or 0.38. If 0.40 is used, the resistance function simplifies to $^1/_{\sqrt{f}} - 2 \log_{10} \frac{r_o}{\lambda}$.

The term $\underline{A}$ is asserted here to be another universal constant, related to the wall zone turbulence. This has not been recognized heretofore and will be seen to have very significant consequences. It is obvious that $\underline{A}$ is constant for a given conduit and roughness type, since it is merely the value of $\frac{v}{v_*}$ in the core velocity distribution at $y = \lambda$, and since $\frac{v}{v_*}$ at any constant value of y is independent of R and R_w. The magnitude of A may easily be scaled off the dimensionless velocity distribution plot at the ordinate $y = \lambda$.

Consider now the situation for some other arbitrary roughness, with the same value of λ as the first roughness but otherwise with different dimensions and shape. Now assume that the flow velocity is adjusted to the point where the phenomena of separation on the roughness elements are mechanically similar to the corresponding phenomena for flow at some given value of R or R_w on the first roughness. In general this would require a different value of R_w than used for the first roughness, but it is apparent that such a similar condition could be produced. The location of the separation point on the roughness elements can be adjusted by adjusting R. The turbulence phenomena in the wall zone (beyond the roughness crests, of course) depend primarily and directly on the character of the wakes rather than the form of the elements producing the wakes.

Assuming then that the wake and wall turbulence phenomena at some value of R_w for the second roughness are made mechanically similar to those for the first roughness at some other value of R_w, the $\frac{v}{v_*}$ distributions for the two situations must be similar in the wall zone. The values of ψ, c, and A_w would therefore be equal in the two situations, and this would also mean that the $\frac{v}{v_*}$ distributions in the core would be the same. In other words, the plots of $\log \frac{y}{\lambda}$ vs. $\frac{v}{v_*}$ for the two situations would coincide throughout.

Therefore, the value of $\underline{A}$ can be made the same for the two roughnesses. But since, as we have seen, $\underline{A}$ is constant for any one roughness, it must therefore have the same constant value for both roughnesses. A similar argument could be developed for roughnesses of different λ - values.

The inference, therefore, is that the term $\underline{A}$ is independent of surface roughness. Its magnitude may be determined by scaling $\frac{v}{v_*}$ from any core velocity distribution curve, at a distance $y = \lambda$ from the roughness crests.

This in turn means that the limiting value of the resistance function, $\frac{1}{\sqrt{8}} (A - \frac{3}{2k})$ is also a universal constant, independent of surface roughness. Its magnitude, as well as the magnitude of $\underline{A}$ will be determined shortly from the available experimental data.

First, however, the implications of the additive term should be noted. In the regime in which the corrective term has not yet vanished, its magnitude continuously decreases as the wall Reynolds number increases. An analysis of equations (11) and (14) will show that this in turn means that for wake-interference flow in any given pipe the friction factor must increase with increasing Reynolds number, becoming and remaining constant when the corrective term vanishes.

The corrective term, in the case of axial flow, may conveniently be simplified to $\frac{2}{\sqrt{8}}\left(\frac{1}{k} - \Psi\right)\left(\frac{c\lambda}{r_o}\right)$, since the term $\frac{1}{2}\left(\frac{c\lambda}{r_o}\right)^2$ would almost always be negligible compared to the term $2\left(\frac{c\lambda}{r_o}\right)$. For a given value of the wall Reynolds number, the expression $\left(\frac{1}{k} - \Psi\right)$ will depend only on the form of roughness element. The term $\left(\frac{c\lambda}{r_o}\right)$ is simply a ratio of two radial dimensions, the distances from the roughness crests to the break in the velocity distribution curves and to the pipe center. It is reasonable to think that these dimensions would be geometrically similar for a given roughness form, and thus that their ratio would be independent of the relative roughness spacing $\frac{r_o}{\lambda}$.

Consequently, the corrective term may be considered as primarily a function of the wall Reynolds number R_w, and the cross-sectional form of the roughness elements. This means that, if the resistance function $\left(\frac{1}{\sqrt{f}} - 2\log_{10}\frac{r_o}{\lambda}\right)$ is plotted against the wall Reynolds number, $\left(\frac{R\sqrt{f}}{r_o/\lambda}\right)$, a single curve should result for each form of roughness element. Furthermore, the curves for all forms of roughness will approach and reach the same limiting value of the resistance function $\frac{1}{\sqrt{8}}\left(A - \frac{3}{2K}\right)$. The value of R_w at which the corrective term vanishes would be expected to depend on the form of the roughness elements.

Velocity Distribution Data in Wake-Interference Flow

There are available several sets of experimental velocity distribution data on conduits of regular surface roughness pattern. However, most of these test conduits were of rather small size.

The only applicable velocity distribution data on large pipes of which the writer has knowledge are a series of measurements made at the St. Anthony Falls Hydraulic Laboratory on 24 inch and 36 inch diameter corrugated metal pipes (9). The two pipes were each 193 feet long. In all, some fifteen velocity distribution curves were obtained at sections at which the turbulent boundary layer was fully developed. A few typical curves are shown on Fig. 1.

When plotted with $\frac{v}{V_*}$ as abscissa and $\log_{10}\frac{y}{\lambda}$ as ordinate, these curves all indicated a definite break between the wall and core velocity distribution curves. From these plots, the values of $\underline{k}$, $\underline{\Psi}$, and $\underline{A}$ were measured and plotted with the wall Reynolds number as common abscissa.

The value of $\underline{A}$ was found to vary only slightly from its average value of 8.70, the range of values being from 8.4 to 9.3, and the standard deviation 0.24. In view of all the possible causes of data dispersion, this appears to

demonstrate satisfactorily the essential constancy of the number $\underline{A}$ for corrugated pipe at a value close to 8.70.

Similarly, the values of $\underline{k}$ were found to be fairly constant, with an average value of 0.36, and standard deviation of 0.03. The scatter of values of both A and k about their means was essentially random.

However, it was evident that the parameter Ψ increased with increasing values of R_w. The scatter of the data was such that any curvilinear relationship could not be detected. The straight-line regression equation for this relation was:

$$\Psi = 1.00 + \frac{R\sqrt{f}}{155{,}000\ r_o/\lambda} \qquad (13)$$

It is probable that the assumed straight line would curve over at high values to become tangent to the line $\Psi = \frac{1}{k}$. The minimum value of R_w at which this would occur could be computed by extrapolation of eq. (13) to the value of $\Psi = \frac{1}{.36} = 2.77$. This computation yields the very high value of 274,000 for the smallest value of R_w at which the limiting resistance function might be reached. Since the maximum experimental value attained for the latter was 67,000, it is obvious that very high velocities would have to be reached before a constant condition could be established.

This means also that the friction factor must continue to increase as the Reynolds number increases, to very high values of the latter, for corrugated surfaces. It will be seen shortly that experimental results of friction tests on these pipes confirm this implication.

Turning now to consideration of other pertinent velocity distribution data that have been obtained by various experimenters, results from the work of Nikuradse (11), Schlichting (13), and Vanoni (19), will be briefly examined.

The tests of Nikuradse on pipes roughened by densely-packed uniform sand grains have hitherto been interpreted in terms of the relative roughness, $\frac{r_o}{h}$. However, it is evident that the relative roughness spacing $\frac{r_o}{\lambda}$ was numerically equal to $\frac{r_o}{h}$ in his pipes, so that either parameter could be used without affecting any of his numerical results. The Nikuradse rough-pipe velocity distribution equation can therefore be written:

$$\frac{v}{V_*} = 8.5 + \frac{1}{k}\log_e \frac{y}{\lambda} \qquad (14)$$

The value of A for surfaces densely packed with uniform sand grains is therefore about 8.5. Thus, two pipe surfaces as radically different in character as corrugated metal and sand give practically identical results for the generalized velocity distribution equations. This is strong confirmation of the significance of the roughness spacing in the flow structure. No such correlation as this is at all possible on the basis of the roughness height.

The tests of Schlichting included many different types of roughness elements, installed on test plates which were arranged to form one side of a rectangular conduit in which two-dimensional flow was obtained near the transverse center of the plate. Most of his test plates produced isolated-roughness flow, and will be mentioned later, in the discussion of that type of flow. Three plates, however, evidently produced wake-interference flow.

One of these was a plate coated with dense uniform-grain sand, 0.135 cm. in diameter. Another was a plate to which were attached spheres 0.41 cm. in diameter and with a spacing of 0.60 cm. in both directions. The third plate had angles extending transversely throughout the plate width, 0.30 cm. high, and spaced at 2.00 cm. intervals.

Schlichting published velocity distribution curves for all his roughnesses. Though the tests were all made at high values of R_w, making the breakpoint in the velocity distribution curves difficult to determine closely, the latter all revealed a definite decrease in slope in the wall zone.

After correcting Schlichting's data and curves to a datum at the roughness crests, then determining $\underline{A}$ as the value of $\frac{v}{V*}$ at $y = \lambda$, it was found that the sand roughness plate and sphere roughness plate gave 7.8 for A; the plate with long angles gave 8.2 for A. These values are not very different from the $\underline{A}$-values obtained in the Nikuradse and St. Anthony Falls pipes. They are consistently lower, however, which probably reflects the two-dimensional structure of the flow.

The velocity distribution data of Vanoni were obtained in a rectangular open channel, with a bottom surface composed of densely packed sand, 0.88 mm. in diameter. The published velocity profiles were taken at the center line, where the flow was two-dimensional. Those which are pertinent here consist of the three runs made with clear water (most of his data involved silt-laden flows).

The boundary between the center and wall zones was quite distinct, occurring at a distance of about $y = 10\lambda$. This large value of $\underline{c}$ ($\underline{c}$ was of the order of magnitude of unity for the St. Anthony Falls pipes and the Schlichting conduits) appear merely to confirm the deduction that $\underline{c}$ should be large for small values of λ/r_o.

The $\underline{A}$ - values for Vanoni's three curves are found to be approximately 8.0, 6.8, and 7.7, with an average of 7.5. This is very near to the values of $\underline{A}$ in two-dimensional flow found for Schlichting's three test plates, the slight difference perhaps being attributable to free surface effects.

The available velocity distribution data, though limited, thus seem to support the previous theoretical inference that the term $\underline{A}$ should be a universal constant, independent of the type of wall surface. A small difference due to cross-sectional form seems to exist, however. For axial flow, $\underline{A}$ is about 8.7 and for two-dimensional flow about 7.8.

Numerical values for $\underline{A}$ and $\underline{k}$ can now be inserted in the generalized resistance equations (11) and (12). If $\underline{k}$ is assumed to be 0.40, for simplicity, and $\underline{A}$ is taken as 8.7, and 7.8 for axial and two-dimensional flow, respectively, these equations become, respectively:

$$\frac{1}{\sqrt{f}} - 2 \log_{10} \frac{r_o}{\lambda} = 1.75 + \frac{\sqrt{2}}{2} \left(\frac{C\lambda}{r_o}\right) \left(2.5 - \psi\right) \tag{15}$$

$$\frac{1}{\sqrt{f}} - 2 \log_{10} \frac{b}{\lambda} = 1.75 + \frac{\sqrt{2}}{4} \left(\frac{C\lambda}{b}\right) \left(2.5 - \psi\right) \tag{16}$$

It is very interesting, though probably fortuitous, that the limiting value of the resistance function in both axial and two-dimensional flow is 1.75. Since most other cross-sectional shapes could probably be referred to a circular section through use of the hydraulic radius ($r_o = 2R_h$), the number 1.75

appears to be a most remarkable universal constant, independent of both surface roughness and cross-sectional form.

Experimental Verification of the Generalized Resistance Equation for Wake-Interference Flow

It has been seen that such velocity distribution data as are available for the wake-interference type of flow support the general theoretical relations developed previously. However, these data are limited, and much stronger confirmation of the theory can be obtained from the available friction loss data in conduits with surface patterns of roughness producing this type of flow.

Eqs. (15) and (16) indicate that, for wake-interference flow, the resistance function decreases from some maximum value to a minimum value of 1.75 as R_W increases. This transition would be expected to have a form depending upon the form of roughness elements, but the limiting value of 1.75 would be applicable to all types of roughness elements. The maximum possible value of the resistance function could be estimated by assuming a ψ of zero, and a value of $\frac{c\lambda}{r_o}$ of unity. These values would give 3.52 as the maximum possible value of the resistance function (2.64 for two-dimensional flow). The maximum value for any particular type of roughness may be less than this, but it cannot be greater. The equation further implies that the friction factor will increase as the Reynolds number increases, for any given value of $\frac{r_o}{\lambda}$. Also, for a given Reynolds number, the friction factor increases as $\frac{r_o}{\lambda}$ decreases.

The foregoing description of the transitional zone and limits for wake-interference flow comprises a rigorous set of specifications which experimental data must fulfill. However, it will be seen that every feature of these specifications is supported by a great variety of data, obtained by many different experimenters, working under many different conditions and with many types of conduits, including both pipes and open channels.

These data can best be analyzed when plotted with the resistance function as ordinate and the wall Reynolds number as abscissa. A logarithmic scale is used for the latter, because of the large range of values involved. The ordinates are plotted increasing downward in order to emphasize the similar appearance of this type of plot to the more familiar f - R plotting.

First the data available for corrugated strip roughnesses will be examined. Tests on several commercial corrugated metal pipes have been carried out at the St. Anthony Falls Hydraulic Laboratory (14), (16). The tests included 18", 24", and 36" diameter circular pipes and 18", 24", and 36" pipe arch sections. The corrugations had a spacing λ of 2 2/3 inches and height $\underline{h}$ of 1/2 inch.

It can be shown that these data strikingly exhibit the phenomena associated with wake-interference flow. Fig. 2 shows the resistance function plotted against the wall Reynolds number for these tests. The strong conformity of the data from all pipes to one curve is evident. The resistance function is seen to decrease gradually from about 2.7 to about 1.9, over a range of R_W from about 7,000 to 60,000. The limiting value of 1.75 was not reached, but the curve gives every indication of a tangential approach to this limit as a value of R_W of probably about 350,000. This is essentially the same inference deduced from the ψ - R_W curve for the corrugated pipe velocity distributions

discussed previously. The friction data for part-full flow in these pipes were also found to lie on the same curve although with somewhat more dispersion.

There are a few other sets of experiments on corrugated pipe surfaces of importance here. Gibson (4) made tests on a 2-inch copper pipe, with sine wave corrugations of $\lambda = 0.4$ inch and $h = 0.1$ inch. Streeter (17) made tests on two corrugation type roughnesses, numbered IV and VI in his notation. The tabulations of data published by Gibson and Streeter had to be recomputed on the basis of a datum at the roughness crests, and this was also true of most of the other published data on other types of roughness.

The combined data from the results at the St. Anthony Falls Laboratory and those of Gibson and Streeter are plotted on Fig. 3. They define almost the complete transition curve from smooth pipe flow to quadratic-law turbulent flow. The curve is valid for a wide range of values of λ, h, and r_o, for both circular and deformed sections and for both pipe and open-channel tranquil flow.

Other tests on corrugated metal pipes, such as those performed by Yarnell, Nagler, and Woodward (20), did not include measurements of water temperature, making it impossible to compute accurate values of R or R_w. However, the range in resistance function was about the same as in the St. Anthony Falls Tests.

Fig. 4 contains resistance function data based on experiments on surfaces containing uniform spot-type roughness elements. These data include the familiar Nikuradse sand surface plot, the Schlichting sand roughness and spherical roughness previously described, and two roughnesses tested in an open channel by Bazin (1) and discussed by Keulegan (8). One of these roughnesses was composed of fine gravel, the other of coarse gravel.

Fig. 5 shows data for sharp-edged strip roughnesses. These include data obtained by Streeter (17) on two strip roughnesses composed of threads cut in a 2-inch brass pipe. One of these was trapezoidal in cross-section with $\lambda = 0.0435$ inches and $h = 0.012$ inches (Roughness V in his terminology). The other was rectangular, with $\lambda = 0.087$ inches and $h = 0.022$ inches. Also included are data obtained more recently by Streeter and others at Illinois Institute of Technology (18) on two square thread roughnesses in a 4.5 inch aluminum pipe. Schlichting's angle roughness plate, referred to previously, is included. Also a surface tested by Fage (3) composed of staggered, square-based pyramids, is applicable here, since the pyramid edges formed what was essentially a sharp-edged strip roughness pattern.

Finally, the approximate curves for all the data plotted on Figs. 2 through 5, have been brought together in one plot on Fig. 6. This assemblage of curves strikingly delineates the nature of wake-interference flow, confirming all the theoretical implications previously noted. Each major roughness type produces a resistance function curve which departs from the smooth-pipe curve at a value of the resistance function equal to or less than 3.5, and then gradually decreases to the minimum value of 1.75, remaining constant thereafter. The limiting value is reached soonest for spot roughnesses, next for sharp-edged strip roughnesses, and last for rounded strip roughnesses.

Thus, the theory of wake-interference flow as developed previously, appears to be adequately substantiated by the available data. Furthermore, the curves of Fig. 6, judiciously applied, may also be used to predict friction factors for this type of flow in conduits of almost any regular roughness pattern.

Isolated-Roughness Flow

This type of flow is characterized by independent development and dissipation of form turbulence behind each element, and by friction drag turbulence along the wall between the elements. The over all pattern of flow will be intermediate between smooth-pipe flow and flow following the square law. The friction factor would decrease with increasing Reynolds numbers, and in some instances might approach or reach a constant value at high Reynolds numbers.

As a reasonable approximation, the total drag force may be written as a summation of wall friction drag and roughness element form drag, as follows:

$$\Delta p\,(A) = \tau_w L_p + 1/2\,\rho\, C_D V_w^{\,2}\, \frac{L}{\lambda}\, h\,(p - ns) \tag{17}$$

where $\underline{\Delta p}$ is the pressure drop in length $\underline{L}$, $\underline{A}$ is the area of flow cross-section, $\underline{\tau_w}$ is the wall shearing stress, $\underline{p}$ is the wetted perimeter, $\underline{\rho}$ the fluid density, $\underline{h}$ the roughness element height, $\underline{C_D}$ the drag coefficient for the element, $\underline{n}$ the number of individual elements in a periphery, $\underline{s}$ the clear transverse spacing between elements, and $\underline{V_w}$ the flow velocity at the roughness crests.

If $\underline{f}$ is the bulk friction factor and $\underline{f_w}$ is the friction factor for the wall surface alone, this equation can easily be shown to reduce to

$$f = f_w + \frac{4C_D}{\lambda/h}\left(\frac{V_w}{V}\right)^2\left(1 - \frac{ns}{p}\right) \tag{18}$$

Assuming the wall surface to be essentially smooth, it has been shown by Nikuradse that $\left(\frac{V_w}{V}\right)^2 = 16.8\, f_w$. As an approximation, this relation may be introduced and equation (18) then becomes:

$$f = f_s\left[1 + \frac{67.2\, C_D}{\lambda/h}\left(1 - \frac{ns}{p}\right)\right] \tag{19}$$

This equation indicates the nature of isolated roughness flow. The friction factor is obtained by multiplying the smooth pipe friction factor by a coefficient greater than unity, the excess depending on the roughness index $\underline{\frac{\lambda}{h}}$, the drag coefficient C_D and the proportion of normal wall length intervening between roughness elements around the periphery to the total wetted perimeter, $\frac{ns}{p}$. For strip roughnesses, $ns = 0$.

As a general check on the validity of equation (19), reference will be made to the various test roughnesses of Schlichting (13). These roughnesses included spheres (two sizes), spherical segments, cones, short angles and long angles, each tested for various values of $\underline{\lambda}$ and $\underline{s}$.

These plates, with four exceptions, produced isolated roughness flow. Three of them produced wake-interference flow and have already been discussed. One produced skimming flow. The measured friction factors on the plates giving isolated roughness flow agree very satisfactorily with friction factors computed from eq. (19).

Considering also this type of flow in open channels, reference may be made particularly to the data of Powell (12), who tested flows over various arrangements of 1/4 inch and 1/8 inch square battens on the bottom and sides

of a rectangular flume. Again a comparison of measured friction factors with values computed from eq. (19) indicates excellent agreement. It is interesting that this agreement is obtained for both tranquil and rapid (though not "ultra-rapid") flows.

The detailed tabulations of these computed and observed values of "f" are not included herein for want of space, but are available elsewhere (9) for those interested.

It is believed, therefore, that the concept of isolated roughness flow harmonizes with the data of Schlichting and Powell, and that eq. (19) therefore gives a good representation of this type of flow.

Quasi-Smooth Flow

For surfaces with very low roughness indices, the flow will more or less skip over the crests of the roughness elements. Between the elements will be regions of dead water, with stable vortices set up in these regions by the moving fluid above the elements. The combination of the roughness crests and the still water in the interstices serves as a pseudo-wall, probably somewhat wavy in character but without large roughness projections. Consequently, this type of flow has been called "quasi-smooth" or "skimming" flow.

Vortex generation at the hypothetical smooth wall is the predominant source of turbulence in the bulk flow. However, maintenance of the stationary eddies between the elements probably requires expenditure of more of the available energy. As an approximation to the energy balance involved, it may be reasonably assumed that the total energy consumed is equal to the energy that would be required to maintain flow in a smooth pipe plus that required to maintain the groove eddies.

These eddies can be regarded as essentially rectilinear circular vortices, of diameter equal to $\underline{j}$, the width of groove (or $\underline{h}$, the depth, whichever is smaller) and of length equal to the conduit perimeter $\underline{p}$. The velocity at the vortex perimeter is equal to a coefficient $\underline{C_w}$ times the wall velocity of flow $\underline{V_w}$. The angular velocity ω is constant at any radius.

The energy of flow per unit time through any concentric cylindrical shell of the vortex is:

$$dE = \frac{1}{2}(dm)\,v_r^{\,2} = \frac{1}{2}\;\rho\, p(dr)v_r^{\,3}$$

$$= \frac{1}{2}\;\rho p(dr)\,(\omega r)^3 = \frac{1}{2}\;\rho\;p\;\frac{(c_w\,v_w)^3}{\left(\frac{j}{2}\right)^3}\;r^3\;(dr) \qquad (20)$$

The total vortex energy is:

$$E = 2\int_0^{j/2} \frac{\rho p(c_w v_w)^3 \cdot 8}{2\,j^3}\, r^3\, dr = \frac{\rho p j (c_w v_w)^3}{8} \qquad (21)$$

The head expended in a length of pipe $\underline{L}$ due to these groove vortices is therefore:

$$H_v = \frac{\rho p j (c_w v_w)^3}{8}\;\cdot\;\frac{1}{AV\nu}\;\cdot\;\frac{L}{\lambda} = \frac{L}{4R}\;\frac{V^2}{2g}\;\frac{j}{\lambda}\left(\frac{c_w v_w}{V}\right)^3 \qquad (22)$$

where $Av\,\nu$ is the weight of fluid flowing per unit time. Adding the head loss in a smooth-pipe, and simplifying, the resulting bulk friction factor is therefore:

$$f = f_s + \left(\frac{c_w v_w}{V}\right)^3 \frac{\lambda}{(j,h)} \qquad (23)$$

In the roughness index term, $\frac{\lambda}{h}$ or $\frac{\lambda}{j}$ would be used depending on whether h or j were smaller. The coefficient c_w would have to be somewhat smaller than unity, perhaps of the order of magnitude of $\frac{1}{2}$. The ratio $\frac{v_w}{V}$ would also be of this general order of magnitude.

In many cases the additive term would be practically constant, and the f-R curve would be roughly parallel to that for smooth pipes (apparently diverging somewhat if plotted on a logarithmic scale, of course).

On the other hand, if there is a slight increase in $\frac{v_w}{V}$ with increasing R, as seems possible, the additive term will be increased materially because of the cubing operation required. Consequently, for many roughnesses, the friction-factor curve in skimming flow may be expected to diverge somewhat from the smooth pipe curve at high Reynolds numbers.

The best available experimental data on skimming flow appear to be those obtained at Illinois Institute of Technology under the direction of Streeter (18). Friction loss and velocity distribution measurements were made on three geometrically similar square-thread roughnesses cut into a 4 1/2 inch dia. pipe. The pertinent dimensions are given on Fig. 7.

Note that the roughness index was the same for all three roughnesses, although the relative roughness was made to vary considerably. Eq. (23) indicates that the friction factor should be independent of the relative roughness, but should depend on the roughness index. Fig. 7, showing the f-R curves obtained on these pipes, shows the curves to be essentially coincident, just as implied by eq. (23). The curves also follow the implied trend of more or less paralleling the smooth-pipe curve, but finally diverging from it and evidently becoming essentially horizontal.

The marked difference between these curves and those for the two other I.I.T. roughnesses (roughnesses II and III, shown on Fig. (5), may be noted in passing. The roughness elements for the two latter were identical in every way with roughnesses I_m with the sole exception of the spacing λ, which was large enough to develop wake-interference flow, with its typical rising friction factor characteristic.

The velocity distribution data tabulated in the I.I.T. Report for roughnesses I_l, I_m, and I_s seemed to indicate that $\frac{v_w}{V}$ fluctuated randomly from about 0.62 to about 0.67, with an average of about 0.65. Insertion of this value in eq. (23), together with various corresponding values of f and f_s, then reveals that the coefficient C_w must have averaged about 0.45, with small variation. This is clearly of the right order of magnitude, which gives further support to eq. (23) as providing a satisfactory skimming-flow equation.

The only one of Schlichting's roughness plates to produce skimming flow seems to have been his Plate V, which contained tightly packed spheres 0.41 cm. in diameter. This plate gave materially smaller friction factors than his Plate II, on which the same spheres were placed at a 0.60 cm. spacing, and which has previously been noted to have produced typical wake-interference flow.

In spite of the differences between strip and spot roughnesses, it is interesting to examine the latter in the light of eq. (23) as an approximation. It can be found that a value of $\frac{v_w}{V}$ of 0.65 and for C_w of 0.52 will satisfy Schlichting's experimental results throughout the test range. These values appear quite reasonable.

Though more data are needed, it therefore appears that eq. (23) may prove satisfactory as at least a preliminary quide to the character of skimming flow.

Joint Roughness

Special cases of isolated roughness and skimming flow may be due to the introduction of small-scale vorticity at the pipe or flume joints. If the joint causes a peripheral protrusion into the flow, then the isolated roughness equation (19) applies. If the joint causes a separation between adjacent conduit sections, then the skimming flow equation (23) would be applicable. Both conditions would result in a descending f-R curve, approximately parallel to the smooth-pipe curve.

This phenomenon is illustrated in two sets of experiments conducted at the St. Anthony Falls Hydraulic Laboratory. One was a 4-inch dia. Lucite pipe, with joints at 4.37 ft. intervals (10), the other on three large concrete pipes, 18, 24, and 36 inches in diameter, each with a joint spacing of 6 feet (15). The joints on the 18" pipe were considerably smoother and more snugly fitting than on the 24" and 36" pipes.

All of these pipes were smooth-walled. The concrete pipes had been manufactured by the cast-and-vibrated process, which produces a glossy-smooth surface. The f-R curves for these pipes are shown on Fig. 8, in each case being slightly above and essentially parallel to the Nikuradse smooth pipe curve.

The joint characteristics of the concrete pipes plainly appear in the f-R curves. The 18-inch pipe has the lowermost curve, indicating the best joints. The 24-inch and 36-inch curves were essentially identical and at an approximately constant increment of friction factor above the 18-inch curve. If the turbulence were being determined by the wall surface, as per the Nikuradse-Colebrook equations, the 18-inch curve should lie highest.

Discriminating Criteria for Flow Types

Equations have now been developed for each of the three basic flow types, but there is still the need of adequate criteria for determining which type will prevail in a given situation.

The boundary between wake-interference and isolated-roughness flow can be denoted by equating the resistance functions for the two types of flow. Thus:

$$\frac{1}{\sqrt{f_s\left[1+\frac{67.2C_D}{\lambda/h}\left(1-\frac{ns}{p}\right)\right]}} - 2\log\frac{r_o}{\lambda} = 1.75 + \frac{1}{\sqrt{2}}\left(\frac{1}{k}-\psi\right)\left(\frac{c\,\lambda}{r_o}\right) \tag{24}$$

If the criterion is applied for a Reynolds number of say 2,500,000, for which $f_s = 0.01$, and if the additive term in the right-hand member is assumed to be negligibiy small, the equation simplifies to:

$$\frac{\frac{\lambda}{h}}{C_D\left(1-\frac{ns}{p}\right)}=\frac{67.2}{\frac{100}{\left(2\log\frac{r_o}{\lambda}+1.75\right)^2}-1} \tag{25}$$

This expression would probably prove sufficiently accurate as a discriminating criterion in most cases. The left-hand member involves the roughness element characteristics, the right-hand member the relative roughness spacing. For a given type of roughness element, and a given radius, the equation can be solved by trial for the critical value of the spacing λ which will mark the boundary between isolated-roughness and wake-interference flow.

For example, solution of eq. (25) for Schlichting's long angle roughnesses will be found to yield a critical λ of 1.85 cm. Schlichting's experimental data indicated that wake-interference flow was obtained when this type of roughness had a λ of 2.0 cm., but isolated-roughness flow at higher values of λ.

The spherical roughnesses of Schlichting gave wake-interference flow for a spacing of 0.60 cm., and isolated roughness flow at higher values. The equation indicates the limiting value to be 0.70 cm.

Space does not permit detailed discussion of other data. However, it could be shown that the trends implied by the other available data on various types of roughness elements all are in substantial accord with the implications of eq. (25), which seems, therefore, to serve fairly satisfactorily as a discriminating criterion between isolated-roughness and wake-interference flow. It may also be noted that, for all parameters except λ held fixed, the friction factor increases as $\underline{\lambda}$ decreases in isolated-roughness flow. However, when wake-interference flow is established, a further decrease in $\underline{\lambda}$ results in a decrease in friction factor.

The criterion for differentiating between wake-interference and quasi-smooth flow cannot be set up in a similar way to that above, since the resistance function for quasi-smooth flow does not approach that for wake-interference flow as the λ - value approaches the critical value between the two flow types, but rather moves away from it. The evident implication is that there is a sudden, rather than gradual, change from skimming to wake-interference flow. This sudden change evidently occurs when the stable vortex in the groove gives way to the typical flow separation phenomenon of a continual succession of vortices growing and washing downstream.

It appears likely that this change will occur when the groove width $\underline{j}$ becomes significantly larger than the depth $\underline{h}$. The vortex occupies the entire width of the groove as long as $\underline{h}$ is larger than $\underline{j}$ and therefore can remain stable. But if $\underline{j}$ is much larger than $\underline{h}$, the vortex will adhere to the upstream face of the groove and the stream will flow over and down the vortex against the opposite groove face; this is essentially a typical flow separation action, and the vortex must rapidly become unstable.

This inference appears to be upheld by the available data on skimming flow. The three I.I.T. roughnesses which produced skimming flow all had j/h ratios very slightly greater than unity. The same was true of Schlichting's spherical roughness Plate V, which gave skimming flow.

Flow Over Surfaces of Variable Roughness

The formulas developed thus far have assumed a regular distribution of roughness elements of identical dimensions. A rational analysis is much

more difficult when the several parameters are permitted to vary. However, the three basic types of flow must still exist, and will occur when the roughness patterns satisfy the appropriate criteria. In many cases the best way to estimate friction factors for varied-roughness patterns would probably be to use simple statistical averages of the parameters which vary.

Not many data are available as yet with which to check this assumption. However, the plank roughnesses of Bazin (1) can be considered as a special type of roughness with a repeating pair of λ - values. These planks were equally spaced, but were much wider than their depth. This means that a wake would be produced at both the upstream and downstream edges of each plank, so that the average spacing of wakes was one-half the plank spacing. Bazin's widely-spaced plank roughness consisted of 2.7 cm. by 1 cm. planks, on 7.7 cm. centers. This roughness produced the rising f-R curve characteristic of wake-interference flow, and the limiting resistance function, as computed for the mean spacing (i.e., one-half of 7.7 cm.), can be shown to be approximately 1.78. Similar results can be shown to apply for certain of Johnson's plank roughnesses (7), which evidently produced wake-interference flow. The inference, therefore, is that an average value of λ can be used for non-uniformly spaced roughness elements in the wake-interference flow equations.

Spot roughness elements have been shown usually to produce isolated roughness flow, except when they are packed quite closely. Thus, each element acts independently and the friction factor could presumably be determined by summation of appropriate drag forces on all the individual elements. However, when the roughness elements are closely packed, wake-interference flow is developed. If the roughness elements are predominantly of one size, with only occasional larger elements, the wake-interference phenomena will be controlled by the smaller elements, with isolated-roughness drag forces being added by the larger elements.

These features are illustrated by the data of Colebrook and White (2), who tested various combinations of two sizes of sand coated on a pipe surface, the small grains being densely packed and the large grains in various isolated-roughness patterns. The small grains alone produced an f-R curve with the typical dip-and-rise obtained by Nikuradse and which implies wake-interference flow. The large grains alone gave the typical isolated-roughness descending f-R curve.

The f-R curves for the various combinations seem to demonstrate that the isolated-roughness effects of the large grains controlled at low Reynolds numbers until the smaller grains came into play. Then wake-interference flow was produced, the bulk phenomenon giving a friction factor approximately equal to the friction factor for the densely-packed small grains plus the isolated-roughness value for the large grains.

It can be seen from the Colebrook-White curves that, although wake-interference flow was evidently produced, the dip and rise was considerably flattened by virtue of the isolated-roughness effect of the large grains. It seems likely that this effect would be enhanced by having more than one size of large grain interspersed among the small grains. The inference then is that, for densely packed spot roughness elements with a random size distribution, wake-interference flow would be produced but that the dip-and-rise would be practically eliminated, and that the f-R curve would become and remain horizontal very soon after leaving the smooth-pipe curve. This is, in fact, exactly the result obtained by Harris (5) in tests on pipes coated with stainless steel spray, the resulting surfaces of which were similar to surfaces of densely-packed sand grains of randomly-varying sizes.

Types of Flow Over Commercial Conduit Surfaces

It appears probable that the principles that have been delineated for flow over artificial roughness patterns can be extended to give a rational picture of the flow and resistance phenomena experimentally obtained on commercial pipe and channel surfaces. By far the majority of such pipes exhibit a decreasing friction factor curve, gradually diverging from the smooth-pipe curve.

In many cases, this is attributable to joint roughness, as in the concrete pipes tested at the St. Anthony Falls Laboratory discussed previously. However, most commercial pipe surfaces probably produce typical isolated-roughness elements such as rivets, projecting pieces of aggregate, etc. Frictionfactors for such surfaces should be predictable by means of the isolated-roughness flow equation (19), or in some cases by the skimming-flow equation (23) when the main roughness consists of a joint depression.

Some pipes with very rough surfaces may produce wake-interference flow. In such cases, the typical dip-and-rise of the friction factor and resistance function curves will depend upon the form and degree of uniformity of the roughness elements. Uniform, rounded, elements such as corrugations will result in a deep dip and a long, gradual rise. Closely packed random roughness elements, on the other hand, will produce fully turbulent wake-interference flow almost as soon as the elements begin to pierce the laminar film, so that the friction factor curve will become and remain horizontal soon after leaving the smooth-pipe curve.

Concrete surfaces have, in different tests, been found to give dropping, horizontal, and even rising, f-R curves. This variation obviously results from the wide variation of textures on different concrete surfaces.

Summary and Conclusions

The concept of flow over rough conduit surfaces which has been presented in this paper is based on the assumption that loss of energy in turbulent flow over such surfaces is attributable largely to the formation of wakes (and therefore vorticity "mills") behind each roughness element. The frequency of such vorticity sources in the direction of flow will determine, to a large extent, the character of the turbulence and energy dissipation phenomena in the flow. Therefore the longitudinal spacing of the roughness elements is the roughness dimension of paramount importance in rough-conduit flow.

Under this concept, there must exist three basic types of flow over rough surfaces. These flow types, together with their corresponding equations for friction factor, are as follows:

1. Isolated-Roughness Flow: Flow over roughness elements sufficiently separated from each other so that the vorticity generated at one element is substantially dissipated before it reaches the next element.

$$f = f_s \left[1 + \frac{67.2 C_d}{\lambda/h} \left(1 - \frac{ns}{p}\right) \right] \tag{19}$$

The symbols have been defined previously, and are also given in the Glossary. For this type of flow, the friction factor decreases with increasing Reynolds numbers, and is independent of the radius r_o.

2. **Wake-Interference Flow:** Flow in which adjacent wakes and vortex-deterioration zones interfere with each other, causing a wall zone of abnormal turbulence.

$$f = \frac{1}{\left[2 \log_{10} \frac{r_o}{\lambda} + 1.75 + \frac{1}{\sqrt{2}} (2.5 - \psi) \left(\frac{c\lambda}{r_o}\right)\right]^2} \tag{15}$$

The parameter ψ approaches 2.5 and c approaches zero, so that the last term in the bracketed expression vanishes at some value of the wall Reynolds number $\frac{R\sqrt{f}}{r_o/\lambda}$, the exact depending upon the form of the roughness elements. This means that the resistance function $\frac{1}{\sqrt{f}} - 2 \log_{10} \frac{r_o}{\lambda}$ will approach and reach the same constant value 1.75, <u>for all types of roughness elements</u>. When this regime is reached, the friction factor is independent of Reynolds number, and is inversely dependent on the relative roughness spacing $\frac{r_o}{\lambda}$. Before the constant value is attained, the friction factor increases as the Reynolds number increases.

3. **Quasi-Smooth (Skimming) Flow:** Flow which essentially skims the crests of the roughness elements, with stable vortices in the grooves between the elements.

$$f = f_s + \frac{\left(\frac{c_w v_w}{V}\right)^3}{\frac{\lambda}{(j,h)}} \tag{23}$$

In this type of flow, the friction factor decreases with increasing Reynolds numbers, and is independent of the radius r_o.

The equation for determining whether isolated-roughness flow or wake-interference flow prevails in a given situation is as follows:

$$\frac{\frac{\lambda}{h}}{C_D \left(1 - \frac{ns}{p}\right)} = \frac{\frac{67.2}{100}}{\left(2 \log_{10} \frac{r_o}{\lambda} + 1.75\right)^2} - 1 \tag{25}$$

If the left-hand member exceeds the right-hand member, isolated-roughness flow will occur; conversely, wake-interference flow will occur if the right-hand member exceeds the left-hand member.

The boundary between wake-interference flow and skimming flow is determined by the groove dimensions. When the groove width becomes significantly larger than its depth, then the skimming action will change to wake-interference phenomena.

The concept and the above equations may also be extended to surfaces of variable roughness, usually by merely employing average values of the roughness dimensions which vary. If the surface has roughness elements of such

variety that more than one of the basic flow types would be produced simultaneously, then the friction factors for each flow type can be added to give the apparent friction factor for the surface as a whole.

With regard to typical commercial conduit surfaces, it is apparent that isolated-roughness flow occurs over most of them, including concrete, riveted steel, wood-stave, cast-iron, brick, etc., including also conduits which are nearly smooth but have protrusions at the joints.

Wake-interference flow is obtained on corrugated surfaces, sand or gravel-coated surfaces, and probably in some old cast-iron and concrete pipes. Densely-packed "random roughness" elements will produce wake-interference flow which is fully developed as soon as the "smooth" flow stage is passed.

Skimming flow is obtained in pipes or channels which are nearly smooth but have depressions at the joints.

In general, the expanded concept of rough conduit flow presented in this paper appears to be quite adequately substantiated by experimental data from many different sources. Since it is both comprehensive in scope and also physically reasonable, as well as relatively simple analytically, it is hoped that it may serve as a stimulus to research and to the development of more rational practical engineering design methods in this field. It is suggested that, if the general concept and methods of the paper are adopted by the profession, very useful corollary studies could be directed to the development of devices and methods for making rapid physical measurements of surface roughness characteristics, and to the preparation of design charts or tables based on the various equations presented in the paper.

Acknowledgments

This paper is essentially a condensation of the writer's doctoral thesis (9), to which reference is made for a more detailed elaboration of the new concept and the supporting data. Dr. Lorenz G. Straub, Director of the St. Anthony Falls Hydraulic Laboratory and Head of the Civil Engineering Department of the University of Minnesota, was the writer's adviser during the preparation of this thesis. Dr. V. L. Streeter, Research Professor of Fluid Mechanics at Illinois Institute of Technology, kindly made available to the writer unpublished data obtained under his direction. Others on the Minnesota hydraulics staff, especially Professors Alvin G. Anderson, Edward Silberman and Richard Whittington, and Mr. Thomas Timar have contributed valuable suggestions.

Glossary

A = $(a - \frac{1}{k} \log_e c)$ = the value of $\frac{v}{v^*}$ in the core velocity distribution at $y = \lambda$.

A_w = $(a - \psi \log_e c)$ = the value of $\frac{v}{v^*}$ in the wall velocity distribution at $y = \lambda$.

a = the value of $\frac{v}{v^*}$ at $y = c\,\lambda$, the breakpoint between the core and wall velocity distributions.

b = one-half the distance between the parallel flow boundaries in two-dimensional flow.

C_D = the drag coefficient on an isolated roughness element, approximately the same numerically as for a body of similar size and shape in unconfined flow.

c = a coefficient such that the distance $y = c\lambda$ locates the breakpoint between the core and wall velocity distributions.

c_w = a wall coefficient such that $c_w v_w$ gives the tangential velocity of the upper limb of the groove vortex in quasi-smooth flow.

D = the pipe diameter or equivalent diameter, ft.

e = the uniform sand diameter in the Nikuradse tests, feet.

f = the Darcy friction factor.

f_s = the smooth-conduit friction factor.

f_w = the friction factor due to the wall surface alone, exclusive of effects of roughness element protrusions or depressions.

H_f = the loss of head due to normal internal friction in the flow, feet.

h = the radial height of the wall roughness elements, feet.

j = the width of the roughness grooves in skimming flow, feet.

k = the von Karman universal turbulence constant.

K_s = the equivalent sand-grain size, used as a measure of surface roughness, feet.

L = the length of the conduit reach, feet.

n = the number of individual roughness elements in a typical wetted periphery of conduit.

p = the wetted perimeter, feet.

R = the conduit Reynolds number, $\dfrac{DV\rho}{\mu}$.

R_h = the hydraulic radius, feet.

R_w = the wall Reynolds number, $\dfrac{R\sqrt{f}}{r_o/\lambda}$.

r = the distance from the flow axis to any point in the flow cross-section, feet.

r_o = the pipe radius, measured to the crests of the roughness elements, feet.

s = the clear circumferential spacing between adjacent roughness elements in the periphery, feet.

V = the average velocity of flow in the cross-section, feet per second.

v = the velocity of flow at any point in the cross-section, feet per second.

v_w = the velocity at the roughness crests, feet per second.

v_r = the tangential velocity of any element in the groove vortex in skimming flow, feet per second.

v^* = the shear velocity, $\sqrt{\dfrac{\tau_o}{\rho}}$, feet per second.

y = the radial distance from the roughness crests to any point in the cross-section, feet.

ν = the specific weight of the fluid, pounds per cubic foot.

ψ = the slope of the dimensionless velocity distribution plot in the wall zone in wake-interference flow, that is, $\dfrac{d(\frac{v}{v^*})}{d(\log_e \frac{y}{\lambda})}$.

λ = the longitudinal spacing of roughness elements, feet.

γ = the kinematic viscosity of the fluid, square feet per second.

ρ = the fluid density, slugs per cubic foot.

τ_o = the wall shearing stress, pounds per square foot.

τ_w = the portion of the wall shearing stress due only to friction drag on the wall surface, pounds per square foot.

ω = the angular velocity of the groove vortex in skimming flow, radians per second.

References

(1) Bazin, H.: "Recherches hydrauliques," Mem. divers savants, Sci. Math. et Phys., Vol. 19, Paris, 1865.

(2) Colebrook, C. F., and White, C. M.: "Experiments with Fluid Friction in Roughened Pipes", Proc. Royal Soc. of London, Vol. 161, 1937.

(3) Fage, A.: "Fluid Flow in Rough Pipes", Tech. Report, Aeron. Research Comm., Repts. and Mem. 1585, 1934.

(4) Gibson, A. H.: "The Flow of Water in a Corrugated Pipe" The Philosophical Magazine, Vol. 50, 1925.

(5) Harris, C. W.: "An Engineering Concept of Flow in Pipes" Trans. Amer. Soc. Civil Engineers., Vol. 115, 1950.

(6) Harris, C. W.: "The Influence of Random Roughness on Flow in Pipes", Univ. of Washington Enging. Expt. Station Bulletins, Bulletin 115, 1949.

(7) Johnson, J. W.: "Rectangular Artificial Roughness in Open Channels", Trans. Amer. Geophys. Union, Section of Hydrology, 1944.

(8) Keulegan, G. H.: "Laws of Turbulent Flow in Open Channels", Journ. Research Natl. Bureau of Standards, RP 1151, 1938.

(9) Morris, Henry M.: "A New Concept of Flow in Rough Conduits", A thesis submitted to the University of Minnesota (Minneapolis, Minn.), in partial fulfillment of the requirements for the degree of Doctor of Philosophy, 1950.

(10) Morris, Henry M.: "Preliminary Flow Tests on a Model Culvert", Proj. Rept. 7, St. Anthony Falls Hydraulic Laboratory, 1948.

(11) Nikuradse, J.: "Stromungsgesetze in rauhen Rohren", Forschungscheft, No. 361, 1933.

(12) Powell, R. W.: "Flow in a Channel of Definite Roughness", Trans. Amer. Soc. Civil Engrs., Vol. 111, 1946.

(13) Schlichting, H.: "Experimentelle Untersuchungen zum Rauhigkeitsproblem", Ingenieur-Archiv, Band VII, Heft. I, 1936.

(14) Straub, L. G. and Morris, H. M.: "Hydraulic Data Comparison of Concrete and Corrugated Metal Culvert Pipes", Technical Paper No. 3, Series B, St. Anthony Falls Hydraulic Lab., 1950.

(15) Straub, L. G. and Morris, H. M.: "Hydraulic Tests on Concrete Culvert Pipes" Technical Paper No. 4, Series B, St. Anthony Falls Hydraulic Laboratory, 1950.

(16) Straub, L. G. and Morris, H. M.: "Hydraulic Tests on Corrugated Metal Culvert Pipes", Technical Paper No. 5, Series B, St. Anthony Falls Hydraulic Laboratory, 1950.

(17) Streeter, V. L.: "Frictional Resistance on Artificially Roughened Pipes", Trans. Amer. Soc. Civil Engrs., Vol. 101, 1936.

(18) Streeter, V. L. and Chu, H.: "Fluid Flow and Heat Transfer in Artificially Roughened Pipes", Final Report, Proj. 4918, Armour Research Foundation, 1949.

(19) Vanoni, Vito A.: "Transportation of Suspended Sediment by Water", Trans. Amer. Soc. Civil Engrs., Vol 111, 1946.

(20) Yarnell, D. L., Nagler, F. A., and Woodward, S. M.: "The Flow of Water through Culverts" Univ. of Iowa Studies in Engineering, Bulletin 1, 1926.

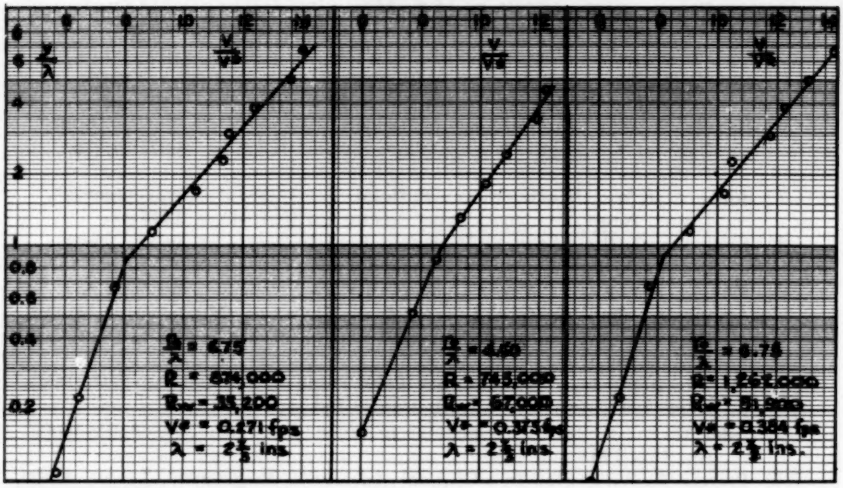

Fig. 1. Typical Velocity Distribution Curves (Corrugated Metal Pipes) $\lambda = 2\ 2/3$

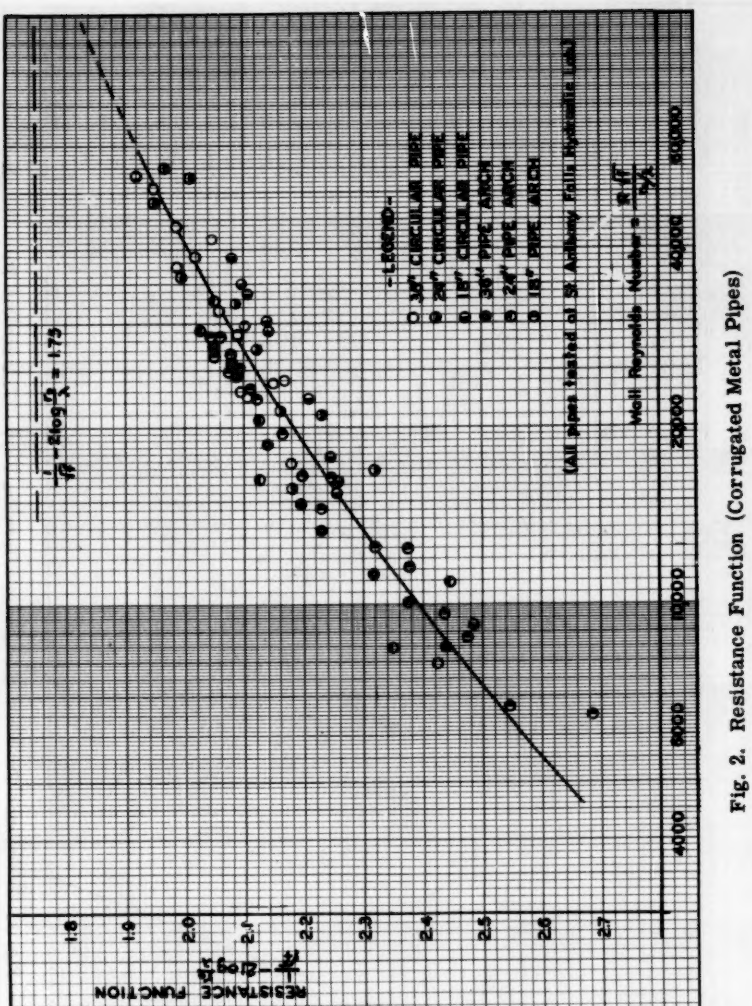

Fig. 2. Resistance Function (Corrugated Metal Pipes)

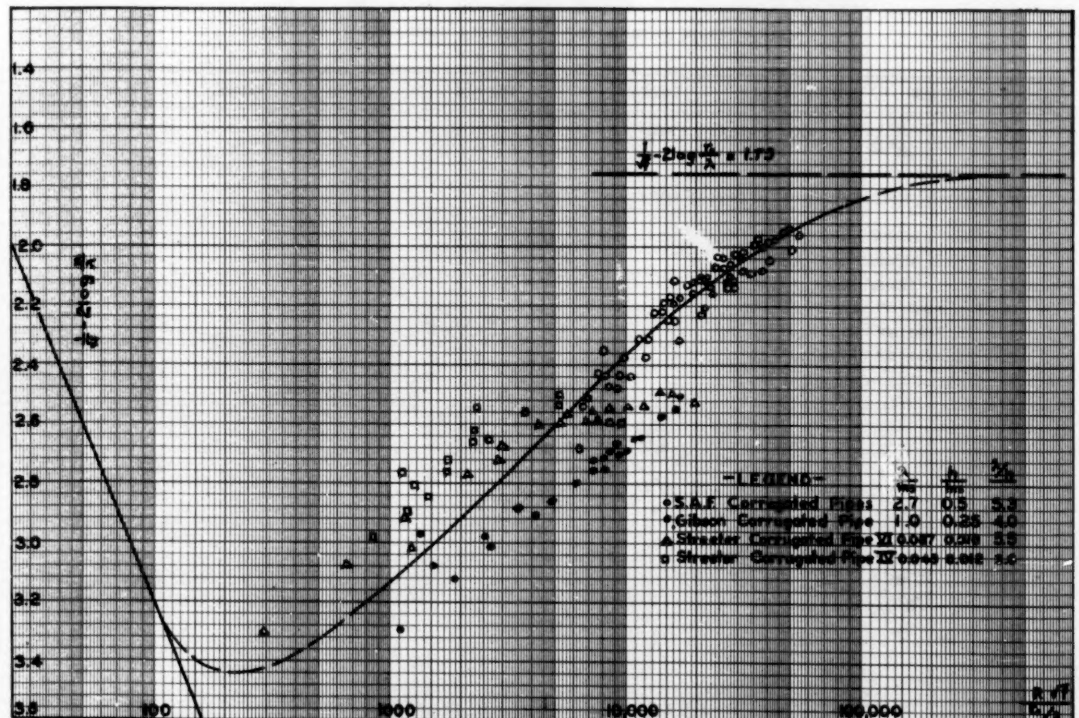

Fig. 3. Resistance Function in Wake-Interference Flow (Corrugation Strip Roughnesses)

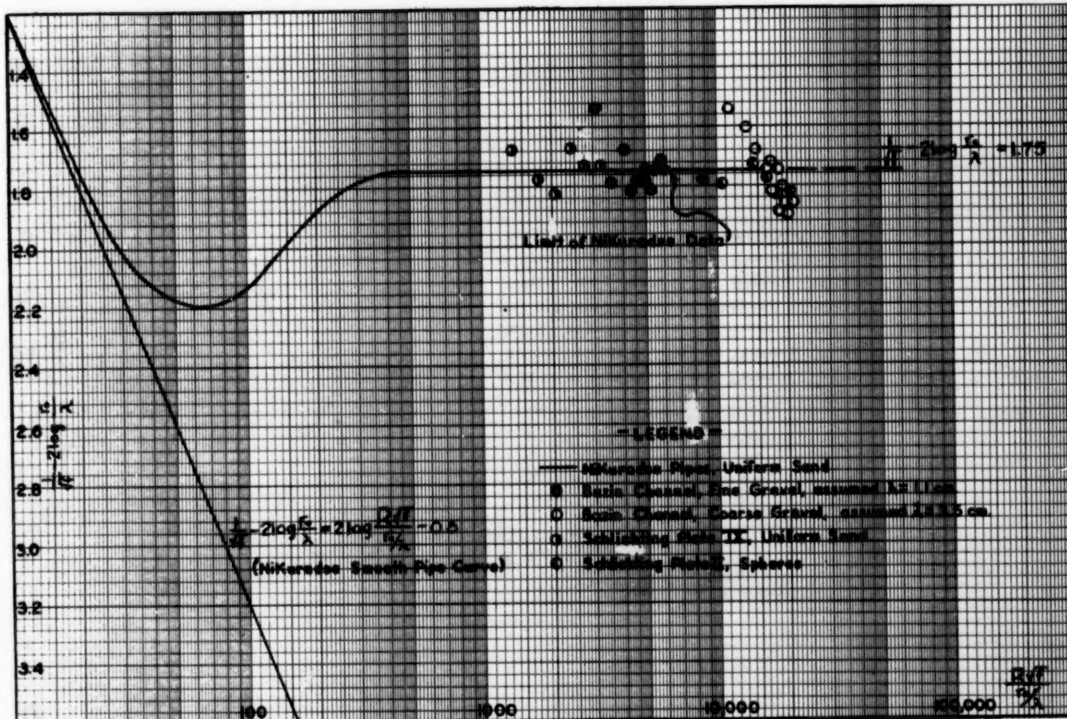

Fig. 4. Resistance Function in Wake-Interference Flow (Uniform Spot Roughnesses)

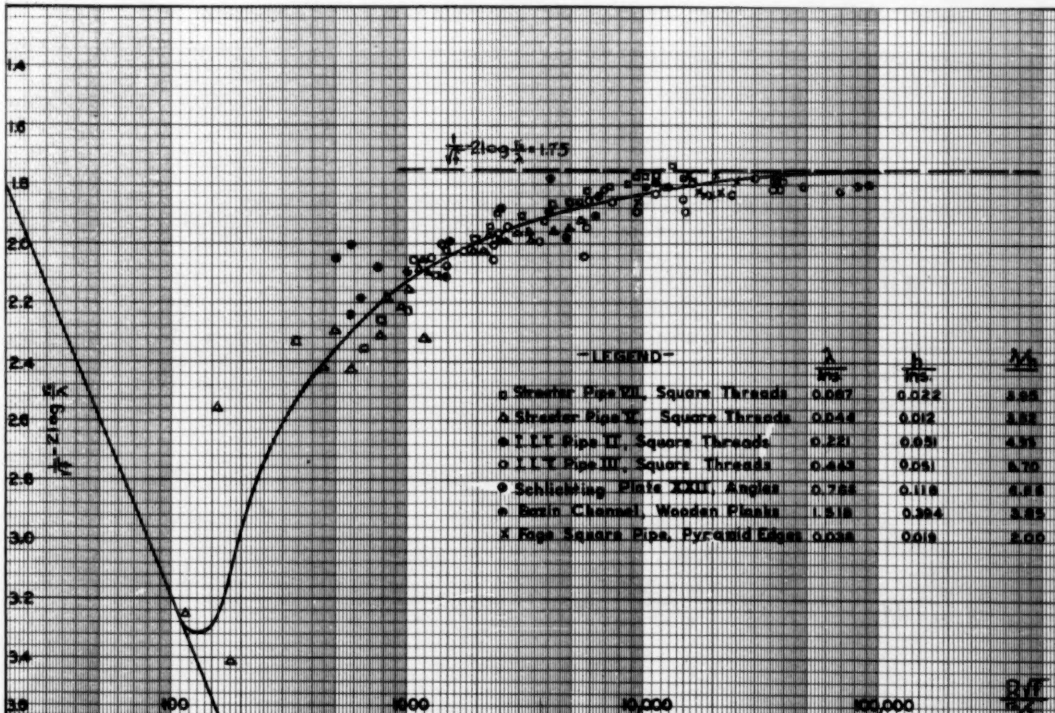

Fig. 5. Resistance Function in Wake-Interference Flow (Sharp-Edged Strip Roughnesses)

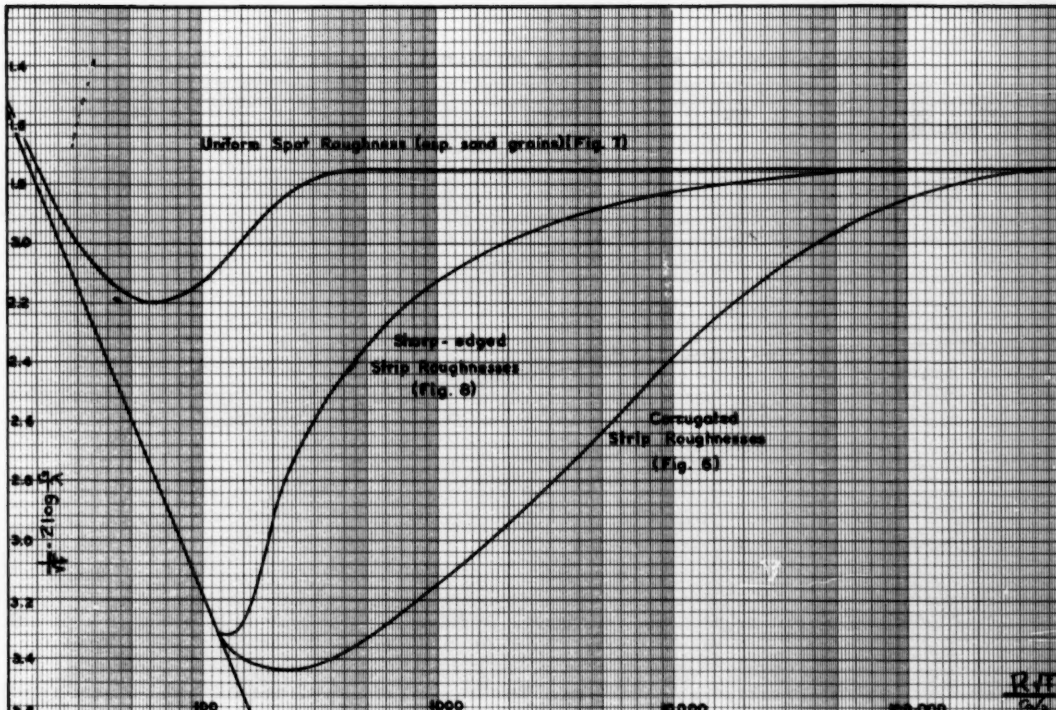

Fig. 6. Approximate Summary Curves for Wake-Interference Flow

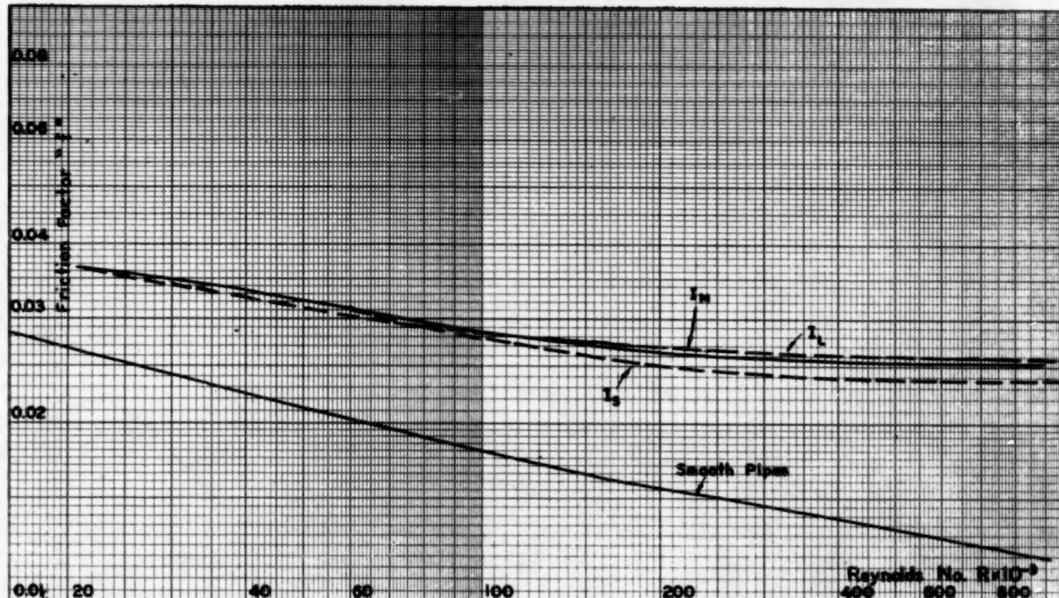

Fig. 7. Friction Factor Curves for Skimming Flow over Square Grooves

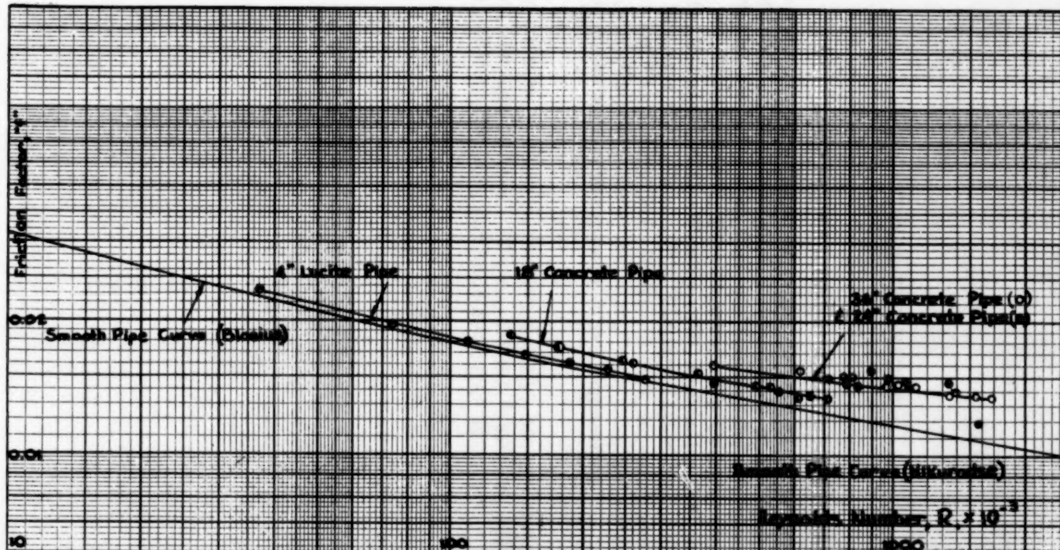

Fig. 8. Friction Factor Curves for Joint Roughness

PROCEEDINGS-SEPARATES

VOLUME 80 (1954)

The technical papers published in the current calendar year are presented below. Technical division sponsorship is indicated by an abbreviation at the end of each Separate Number, the symbols referring to: Air Transport (AT), City Planning (CP), Construction (CO), Engineering Mechanics (EM), Highway (HW), Hydraulics (HY), Irrigation and Drainage (IR), Power (PO), Sanitary Engineering (SA), Soil Mechanics and Foundations (SM), Structural (ST), Surveying and Mapping (SU), and Waterways (WW) divisions. For titles and order coupons, refer to the appropriate issue of "Civil Engineering."

JANUARY: 379(SM),[a] 380(HY), 381(HY), 382(HY), 383(HY), 384(HY),[a] 385(SM), 386(SM), 387(EM), 388(SA), 389(SU),[a] 390(HY), 391(IR),[a] 392(SA), 393(SU), 394(AT), 395(SA),[a] 396(EM),[a] 397(ST).[a]

[a]Discussions grouped by Divisions.

AMERICAN SOCIETY OF CIVIL ENGINEERS

OFFICERS FOR 1954

PRESIDENT

DANIEL VOIERS TERRELL

VICE-PRESIDENTS

Term expires October, 1954:
EDMUND FRIEDMAN
G. BROOKS EARNEST

Term expires October, 1955:
ENOCH R. NEEDLES
MASON G. LOCKWOOD

DIRECTORS

Term expires October, 1954:
WALTER D. BINGER
FRANK A. MARSTON
GEORGE W. McALPIN
JAMES A. HIGGS
I. C. STEELE
WARREN W. PARKS

Term expires October, 1955:
CHARLES B. MOLINEAUX
MERCEL J. SHELTON
A. A. K. BOOTH
CARL G. PAULSEN
LLOYD D. KNAPP
GLENN W. HOLCOMB
FRANCIS M. DAWSON

Term expires October, 1956:
WILLIAM S. LaLONDE, JR.
OLIVER W. HARTWELL
THOMAS C. SHEDD
SAMUEL B. MORRIS
ERNEST W. CARLTON
RAYMOND F. DAWSON

PAST-PRESIDENTS

Members of the Board

CARLTON S. PROCTOR
WALTER L. HUBER

TREASURER

CHARLES E. TROUT

EXECUTIVE SECRETARY

WILLIAM N. CAREY

ASSISTANT TREASURER

GEORGE W. BURPEE

ASSISTANT SECRETARY

E. L. CHANDLER

PROCEEDINGS OF THE SOCIETY

HAROLD T. LARSEN
Manager of Technical Publications

DEFOREST A. MATTESON, JR.
Editor of Technical Publications

PAUL A. PARISI
Assoc. Editor of Technical Publications

COMMITTEE ON PUBLICATIONS

FRANK A. MARSTON

I. C. STEELE
GLENN W. HOLCOMB

ERNEST W. CARLTON
OLIVER W. HARTWELL

SAMUEL B. MORRIS